Modeling Sensor Dependencies between Multiple Sensor Types

Shengfa Miao   MIAO@LIACS.NL
Ugo Vespier   UVESPIER@LIACS.NL
Joaquin Vanschoren   JOAQUIN@LIACS.NL
Arno Knobbe   KNOBBE@LIACS.NL
Ricardo Cachucho   CACHUCHO@LIACS.NL
Leiden University, The Netherlands
Lanzhou University, China

Abstract

With the development of sensing and data processing techniques, monitoring physical systems in the field with a sensor network is becoming a feasible option for many domains. When analyzing data collected from the sensor network, there typically exist substantial correlations between various sensor signals. Employing sensors of multiple types will produce a greater signal variation, but sensors will still be sensitive to related aspects of the measured system, that is to say there are certain dependencies. In this paper, we focus on modeling sensors dependencies among sensor types of a sensor network installed on a Dutch highway bridge. This sensor network is composed of three types of sensors: strain gauges, vibration sensors, and temperature sensors. Through linear regression, convolution, envelope and band pass filters, we succeeded in detecting the dependency between strain gauges and temperature sensors in the time domain, and the dependency between strain gauges and vibration sensors in the frequency domain. To gain insight into these dependencies, and how the placement and location of sensors influences them, we further analysed the obtained models in a secondary analysis step. The methods presented in this paper are demonstrated by means of an application on a highway bridge, but we feel that, due to their general nature, they equally apply to

other domains amenable to sensing.

1. Introduction

With the rapidly decreasing prices for sensors, data gathering hardware and data storage, monitoring physical systems in the field is becoming a viable option for many domains. In fields such as civil engineering, windmills and aviation, so-called Structural Health Monitoring (SHM) systems are becoming popular to understand the actual workings of the system in situ, as well as to monitor the system for any developing faults. More and more, sensor networks consisting of multiple sensor types are being employed in these environments, and large quantities of data are being collected. New methods are required to deal with the proper analysis and interpretation of such data collections. In this paper, we consider a case study of such a multi-sensor network, where non-trivial data processing is required to make sense of the data.

When dealing with multiple sensors measuring a physical system, each individual sensor will be sensitive to some aspects of the system, based on the specific characteristics of the type of sensor and on which part of the system the sensor is placed. This is clearly the case for sensors of different types (such as vibration and temperature sensors), but also for identical sensors attached differently to the system. If two sensors are measuring in each others vicinity, they will likely show some dependency, but in most cases, this dependency will be non-trivial, depending on the location, the orientation and the attachment. As an example, consider an SHM-system employed on an aircraft. In order to measure stresses on a wing, and potential metal fatigue on the wing attachment, *strain gauges* are fitted to the wing attachment. During high-*g*-force

manoeuvres, the strain gauges will measure high values of strain on the attachment. Other sensors might be placed at the tip of the wing, to measure vibrations caused by turbulence for example. These vibration sensors however, will not be sensitive to sustained bending of the wing, as the sensor simply moves along with the wing, and is only sensitive to rapid changes in the location of the wing. As such, strain gauges are sensitive to different aspects of the dynamics than vibration sensors, although some overlap exists in the physical phenomena captured by either type.

In this paper, we provide some examples of modeling the dependencies between (pairs of) sensors, specifically where multiple sensor types are involved. We will demonstrate the methods on data collected at a Dutch highway bridge within the InfraWatch project (Knobbe et al., 2010; Vespier et al., 2011; Miao et al., 2013). The bridge in question is continually being monitored by a collection of sensors of three different types: strain gauges, vibration sensors, and temperature sensors, all sampling at 100 Hz. One of the main challenges here is to understand the specific focus of each sensor type and to model any relationships across types. Having such a model may help, for instance, to remove certain phenomena measured by one sensor type from the signal of another sensor type. Specifically, we will consider the effect of temperature changes on the strain measurements at various locations on the bridge. As such, we can correct for this temperature effect.

Modeling dependencies between sensors also helps to remove redundancies in the data. Being able to infer the measurements of a particular sensor from the remaining sensor may suggest a smaller, and thus cheaper monitoring set-up. Finally, any modeling over the collection of sensors is beneficial for tracking the health of the bridge over longer periods. Changes in the value of a single sensor will often indicate transient effects, such as traffic or weather, but changes in the *models* of the bridge data indicate structural changes to the actual bridge, warranting further investigation.

A further issue we will be investigating is the effect that location and placement of sensors has on their usefulness within the network. For example, if we wish to understand the effect of temperature on strain measurements, it will be relevant to know where and how these two parameters are being measured. By investigating the dependencies between all pairs of sensors from two types (in this case strain and temperature), we hope to discover practical guidelines for the optimal placement of sensors. In Section 6, we perform a secondary analysis step based on Subgroup Discovery

to find key characteristics of sensors in terms of their type, location, mode of attachment and orientation.

2. Preliminaries

In the InfraWatch project, a sensor network with 145 sensors is employed. These sensors are placed along three cross-sections of a single span of the bridge. Each of them is either embedded in the concrete, or attached to the outside of the deck and girders. To measure the strain in different directions on the bridge, we utilize sensors of different types: *vibration sensors* measure vertical motion of the bridge, and *strain sensors* measure horizontal strain caused by deflection of the bridge. In the latter case, we measure strain along both the X-axis and Y-axis. To measure the temperature of different parts of the bridge, we also employ multiple temperature sensors. To formalize this placement, we define each sensor as follows:

Definition 1 (Sensor) *A sensor is a tuple (t, x, y, e, o), where $t \in \{St, Vi, Te\}$ indicates the sensor type (strain, vibration, and temperature, respectively), x and y are its coordinates on the bridge, $e \in \{embed, attach\}$ indicates whether the sensor is embedded or attached to the concrete, and $o \in \{X\text{-}axis, Y\text{-}axis\}$ indicates the orientation of the sensor.*

In the remainder of this paper, we will make substantial use of linear correlations between two signals. Specifically, we will use the (Pearsons's) correlation coefficient as a measure for how related two signals are, modulo a linear transformation between the two. In many cases, the challenging part is the non-linear operations that will have to be performed to the signals, in order to make them congruent. What remains is a simple linear transformation in order to translate the one scale (for example degrees Celsius) to another (for example strain in $\mu m/m$). Using the correlation coefficient allows us to measure the dependency between two features in a manner that is independent of the scale in which a sensor happens to measure.

3. Strain & Temperature

In this section, we study the relationship between two types of sensor: strain and temperature. The sensor network features a total of 91 strain sensors, 44 of which are embedded, and 47 are attached. Of the 20 temperature sensors, one half is embedded in the surface of the deck, and the other half is attached to the underside of the deck.
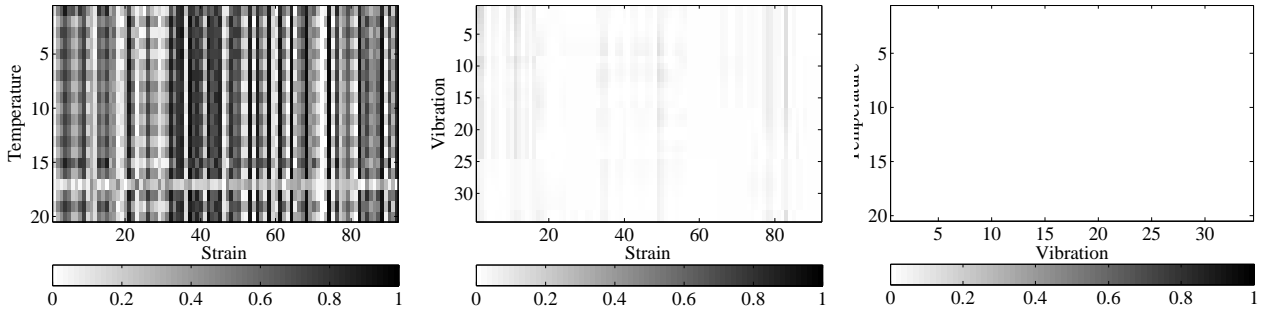
Fig. 1 , the absolute correlation coefficients between

Figure 1. Correlation matrices for St-Te (left), St-Vi (middle) and Vi-Te (right). The numbers on the axes indicate the sensor number.The colorbar value stands for the absolute value of correlation coefficients.

strain and temperature vary from 0 to 0.97. For these sensor pairs with high correlation coefficients, we can simply employ a linear model that assumes the measured strain is directly influenced by the temperature of one of the temperature sensors:

$$S = a \cdot T + b$$

In this model, the coefficients a and b translate between the temperature scale (in Celsius) and the micro-strain scale (in $\mu m/m$). The blue line in Fig.
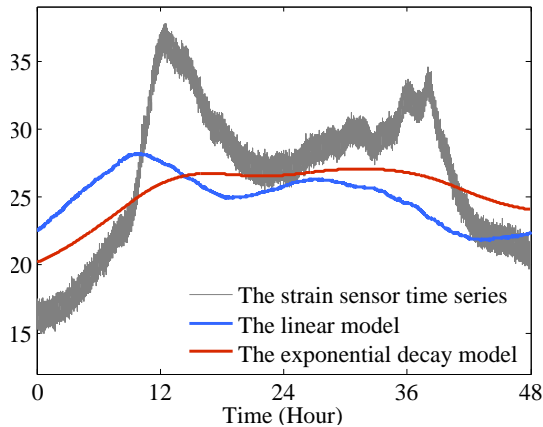

Figure 2. The linear (blue) and exponential decay model (red) between strain and temperature.

2 shows the effect of this model applied to a pair of strain and temperature sensor time series that are only moderately related, with $a = -3.288$ and $b = 27.547$ obtained through linear regression over a longer period of time than displayed here. The correlation coefficient for this example is $r = 0.776$, which indicates that the selected pair of sensors are moderately correlated. However, when considering the time series in more detail, one can note that there is a dependency of the strain signal on the temperature measurements, but this relation is non-trivial: it involves a degree

of delay: the upward and downward movement of the signal appear to be shifted by several hours.

The linear model fails to capture the complete effect of temperature on the strain, because the temperature sensor does not actually measure the bridge temperature, but rather the outside temperature. The temperature of the bridge is of course mostly influenced by the outside temperature, but this influence is spread over time, and the bridge temperature will follow changes of outside temperature with a delay. The amount of delay depends on the size and material of the structure, with larger structures (such as the bridge in question) being less sensitive to sudden changes of outside temperature. In other words, a large concrete bridge has a large capacity to store heat, which is mirrored in a slow response of the strain signal.

In the systems analysis field, systems with a capacity are often modeled as a *Linear Time-Invariant* system (Hespanha, 2009). *Time-invariant* indicates that the response of the system does not change over time, which is a reasonable assumption for a bridge (if subtle deterioration of the structure is ignored). LTI systems are *linear* because their 'output' is a linear combination of the 'inputs'. In terms of the bridge, the temperature of the bridge is modeled as a linear combination of the outside temperature over a certain period of time (typically the recent temperature history):

$$T_{bridge}(t) = \sum_{m=0}^{\infty} h(m)T(t-m)$$

where $T_{bridge}(t)$ is the internal temperature and h is an impulse response (to be defined below). Note that this is a special case of *convolution*, a concept that has been extensively studied in signal processing and analysis (Stranneby & Walker, 2004):

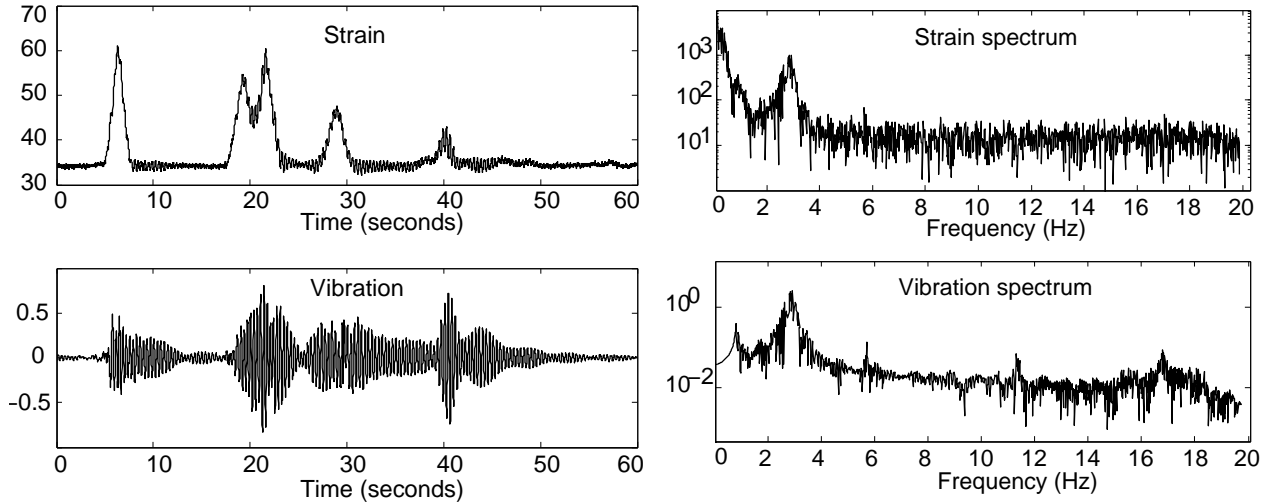$$y(t) = h * x(t) = \sum_{m=-\infty}^{\infty} h(m)x(t-m)$$

Figure 3. Strain and Vibration signal in the time and frequency domain.

Of the many impulse response functions h, which include for example the well-known moving average operation, we decide to model the delayed effect of the outside temperature using the exponential decay function $h_e(m) = e^{-\lambda m}$ (for $m \geq 0$). In this function, λ is the decay factor, which determines how quickly the effect of past values reduces with time. Note that the resulting equation

$$S = a \cdot h_e * T + b, \text{ where } h_e(m) = e^{-\lambda m} \qquad (1)$$

is the solution to a linear differential equation that is known as *Newton's law of cooling*, which states that the change in temperature of the bridge is proportional to the difference between the temperature of the bridge and its environment:

$$\frac{dT_{bridge}}{dt} = -r \cdot (T_{bridge}(t) - T(t))$$

This is a somewhat simplified representation of reality, in that it assumes that the systems consists of two 'lumps', the bridge and the environment, and that within each lump the distribution of heat is instantaneous. Although in reality this is clearly not the case, it turns out that this model performs fairly well.

For a given pair of sensors and the associated data, we will have to choose optimal values for a, b and λ. It turns out that λ behaves very decently, with only a single optimum for given a and b, such that simple optimisation with a hill-climber will produce the desired result. For Equation 1, we obtain a fitted model for the selected sensor pair shown as the red line in Fig. 2, which clearly demonstrates that the exponential decay model has removed the apparent delay in the data. The fitted coefficients were

$a = -12.147, b = 30.463$, and $\lambda = 3 \cdot 10^{-5}$, with a correlation coefficient $r = 0.867$. Considering every possible pair of sensors from St and Te, we find that the correlation coefficients of 47.4% of sensor pairs are improved by the exponential decay model. Indeed, the successful modeling of the dependency for a given pair of sensors still depends on the location and placement of either sensor. In Section 6 we look into the question of finding suitable pairs of sensors in more detail, when we apply Subgroup Discovery to the modeling of St-Te sensor pairs.

4. Strain & Vibration

Our sensor network contains 34 vibration sensors, 15 of which are attached to the bridge deck, while the remaining 19 sensors are attached to the bridge girders. As mentioned in Section 2, both vibration and strain sensors are used to measure the dynamic stresses acting on the bridge. In theory, there should thus be some degree of correlation. However, we failed to detect a strong linear dependency between any pair. As illustrated in Fig. 1 (middle), the correlations between most sensor pairs are quite weak, the highest one for this data being 0.1557. To demonstrate what types of modelling can be done for these two types of sensors, we selected one pair of sensors with a moderate correlation coefficient, as shown in the time domain in Fig. 3 (left). The graphs show that the vibration sensor is a symmetric signal, while the strain sensor time series is not. However, the peaks in both occur consistently, which indicates that they are related. Using a simple correlation, this effect is hidden by the symmetric nature of the vibration signal.
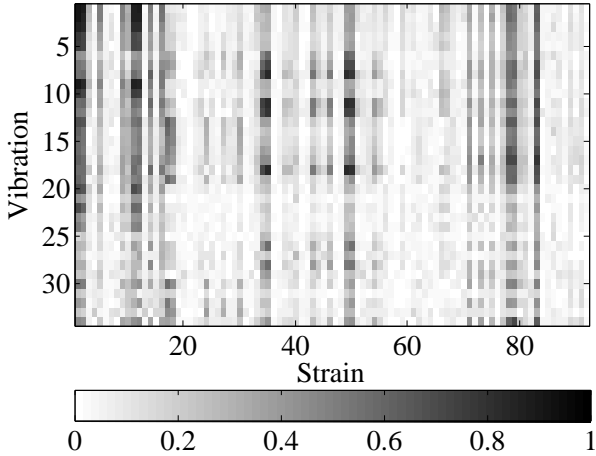
Figure 4. The correlation matrix for St-Vi after applying a band-pass filter in the frequence domain.

Fig. 3, which features the spectra obtained for the two signals by means of a Discrete Fourier Transform (Stranneby & Walker, 2004), shows that despite a lack of a direct relation in the time domain, the signals are actually fairly similar in parts of the spectrum, notably where frequencies above 1 Hz are concerned. Note the big peak around 2.8 Hz in both spectra. In fact, what is missing in the vibration spectrum are the lower frequencies, which correspond to slower bridge movements. In other words, the vibration sensors are not sensitive to gradual changes in the deflection of the bridge, as the sensors themselves simply move along with the bridge. The strain gauges, on the other hand, *are* sensitive even to the slowest changes in bridge deflection. However, both sensors measure shaking of the bridge (frequencies above 1 Hz) in a similar fashion.

Based on these observations, an obvious way to relate St to Vi is to focus on a fairly specific range of frequencies. In our experiments, we have applied a *band-pass filter* to remove all components of the signal outside the range $2.0 - 3.2$ Hz. The linear model between the strain and vibration time series then becomes:

$$BPF_{2-3.2}(S) = a \cdot BPF_{2-3.2}(V) + b$$

in which BPF stands for the band-pass filter operation. After applying the band-pass filter operation to both St and Vi, the correlation coefficient improves from 0.10 to 0.94.

The model we achieved through the band-pass filter operation works well for a small selection of sensor pairs. In Fig. 4, information is displayed on which sensor pairs specifically gain from this operation. Note that some strain gauges correspond well to most of the vibration sensors (dark columns in the matrix). These
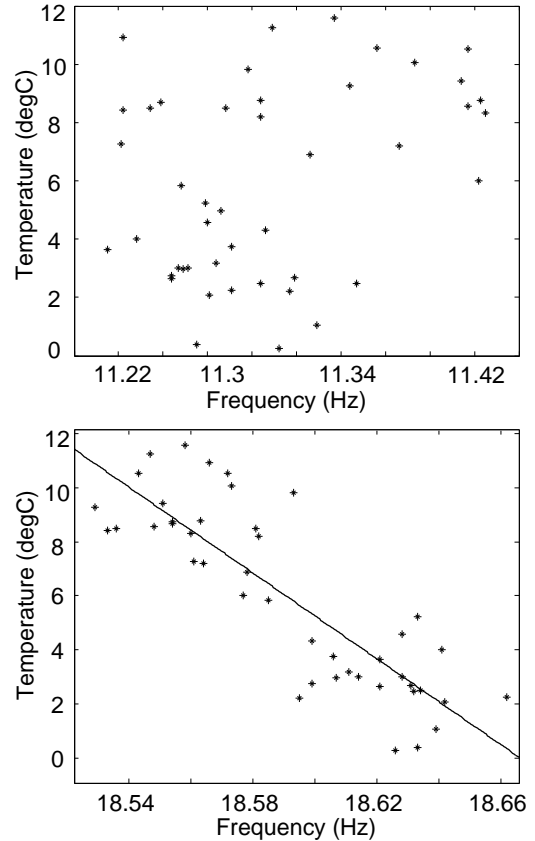

Figure 5. The dependency between modes and temperature.

sensors are primarily located on the right side of the bridge. The few exceptions (St78, St79 and St83) are located on the girder entirely on the other side of the bridge. We look into such observations in more detail in the coming secondary analysis section (Section 6).

5. Vibration & Temperature

As mentioned in the previous section, the vibration spectrum shows little activity in the range below 1 Hz, which happens to be where all of the temperature changes occur (for example due to the daily difference between day and night). For this reason, there are no significant dependencies between the sensors from Vi and Te, shown as Fig. 1 on the right. However, the vibration of the bridge does depend on the temperature. It is well known that bridges tend to oscillate at specific frequencies, and that these frequencies are determined by the stiffness of the structure, which in turn is influenced by changes in the temperature of the material. In a simplified model of a span of the bridge, the *natural frequency* of the span is computed

as follows:

$$f_n = \frac{1}{2\pi}\sqrt{\frac{k}{m}}$$

In this equation, m refers to the mass of the bridge (including the possible load on the bridge), and k is a stiffness coefficient that depends on several factors such as material, humidity, corrosion, etc., but also on temperature. Note that an increasing temperature leads to a decreasing stiffness k, and hence a decrease in frequency, such that we expect a negative relationship between Vi and Te sensors.

The effect of temperature on natural frequencies is widely studied (Song & Dyke, 2006; Xia et al., 2006). After external excitation, for example traffic or wind, a bridge can vibrate in different *modes* (Reynolds & Pavic, 2001). Each mode stands for one way of vibration, which can be vertical, horizontal, torsional or more complicated combinations thereof, and there is one natural frequency corresponding to each. To identify these modes, we use a peak selection method in the spectrum of the vibration sensor (Peeters & De Roeck, 2000). As shown in Fig. 3, we can detect several peaks in the spectrum, each of which is assumed to correspond to a mode. We then consider each mode individually, and look for dependencies between the temperature and the frequency.

In order to consider a substantial range of temperatures, we extracted data from over 45 days, with temperatures between 0 and 12 $°C$. In order to minimize the effect of traffic on m, we selected one hour from each day from 3:00 AM to 4:00 AM. Another motivation for this time-period is the relative stable temperature of both the environment and the bridge. From this hour of data, a spectrum was computed, along with the corresponding modes, as well as the average temperature during this period. Surprisingly, and contrary to many publications (Peeters & De Roeck, 2000; Xia et al., 2006; Liu & Dewolf, 2007; Xia et al., 2011), we find that most modes in the lower ranges of the spectrum (for example the prime one around 2.8 Hz) are not affected by temperature (see Fig. 5 left), at least not in the 12 degrees range available to us. The only mode clearly depending on temperature is around 18.6 Hz, as shown in Fig. 5 right.

6. Analysis of Sensor Properties

As mentioned at the end of Section 3 and 4, we can accurately model some of the strain signals using the temperature signals, and correlate some vibration sensors with strain sensors. However, the models we obtained are not universal for every pair of sensors. To further look into why some sensor pairs work well and others not, we analysed them in a secondary analysis step, where we investigate the influence of various sensor properties such as their location and orientation. The term *secondary analysis* refers to the fact that we are taking the combined set of findings from the previous analysis (the search for sensor dependencies), and treating them as a new data mining task, which is aimed at finding properties of the sensor pairs that help understand why some pairs are easier to model than others. The term *meta-learning* could also apply to this activity.

Our method of choice for this analysis is Subgroup Discovery (SD), which is a descriptive pattern mining technique that aims to outline specific subsets of the data that show a significant deviation of the target, compared to the entire dataset. Our target in this case is the quality of the individual models for sensor pairs (expressed in terms of correlation coefficient), which makes this a regression task. As quality measure for subgroups with a regression target, we use the so-called *(standardized) z-score*, which essentially measures how many standard deviations a subgroup is away from the mean of the entire dataset (see (Pieters et al., 2010) for an overview of quality measures for regression SD). The software we used to conduct these experiment is called Cortana[1], which is a generic toolbox for Subgroup Discovery tasks, including the regression setting that is required here (Meeng & Knobbe, 2011). Any alternative tool for discovering patterns in numeric/nominal data in a regression setting, such as regression trees, would have worked equally well.

Table 1 shows the structure of our data obtained after the initial modeling of sensor pairs. We represent each sensor pair and their properties, including the correlation of the best model, in one row. In the St-Te model we have $91 \cdot 20 = 1820$ rows, and $91 \cdot 34 = 3094$ rows for the St-Vi model. The sensor locations are represented using x and y-coordinates, but in order to allow the SD algorithm to also discover more high-level, interpretable properties, we also introduced several intervals in both dimensions (such as *girder* and *deck* for the y-axis). Additionally, we provided the orientation and type of embedding as nominal attributes.

In our SD run, we search for interesting subgroups with descriptions consisting of conditions on one or more attributes. Although very specific descriptions can be mined, it turns out that fairly simple descriptions are the most informative, so we mine for subgroups of at

---

[1]It can be downloaded from datamining.liacs.nl/cortana.html, and is also available as a plugin for the KNIME package.

Table 1. Example of the data that was used in the secondary analysis.

	STRAIN							TEMPERATURE							CORR.
SENSOR	X	Y	EMBED.	ORIENT.	LANE	LAYER	STRUCT.	SENSOR	X	Y	EMBED.	LANE	LAYER	STRUCT.	
St1	14	0	ATTACH	X-AXIS	RIGHT	GIRDER	GIRDER	Te1	13	7	EMBED	RIGHT	TOP	DECK	0.139
St1	14	0	ATTACH	X-AXIS	RIGHT	GIRDER	GIRDER	Te2	13	5	ATTACH	RIGHT	BOTTOM	DECK	0.024
St1	14	0	ATTACH	X-AXIS	RIGHT	GIRDER	GIRDER	Te3	9	7	EMBED	MIDDLE	TOP	DECK	0.068
...															
St2	14	2	ATTACH	X-AXIS	RIGHT	GIRDER	GIRDER	Te1	13	7	EMBED	RIGHT	TOP	DECK	0.277
St2	14	2	ATTACH	X-AXIS	RIGHT	GIRDER	GIRDER	Te2	13	5	ATTACH	RIGHT	BOTTOM	DECK	0.472
...															

Table 2. The $d \leq 2$ results for the St-Te models ($\mu_0 = 0.533$).

SUBGROUP DESCRIPTION	COVERAGE %	z-SCORE	μ_{S_i}
St vertical = inside deck & St horizontal ≤ 7	11.0	18.2	0.89
St vertical = inside deck & St orientation = Y-axis	9.9	17.8	0.90
St vertical = inside deck	16.5	16.1	0.79
St vertical = inside deck & Te horizontal ≤ 9	13.2	15.9	0.82
St vertical = inside deck & Te horizontal ≥ 5	13.2	14.1	0.79
St vertical = inside deck & Te embedding = attach	8.5	12.2	0.81
St vertical = inside deck & Te horizontal ≤ 5	6.6	11.2	0.82
St vertical = inside deck & Te embedding = embed	8.2	10.6	0.77
St embedding = embed	47.3	10.3	0.63

most two conditions ($d \leq 2$). The algorithm searches for high-quality subgroups using a beam search with beam width $w = 100$ (Meeng & Knobbe, 2011). A z-score-ranked list of subgroups is returned, of which we report the top-ranking results. Note that we filter the final ranking by removing logical redundant subgroups. A minimum subgroup size of 2 was used.

St-Te models The secondary analysis of the strain and temperature sensors takes the absolute correlation value of each sensor pair as the primary target. The first 9 subgroups (sets of pairs of St-Te sensors) are shown in Table 2. The average correlation over the entire set of pairs is $\mu_0 = 0.533$. The columns contain the subgroup description, the percentage of sensor pairs within the subgroup (i.e. the fraction of the database covered), the z-score, and the average correlation with the subgroup, respectively.

This table shows 2 subgroups of depth one and 7 subgroups of depth two. First, we note that the quality of the St-Te models seems to rely mostly on properties of the strain sensors, rather than the temperature sensors. Apparently, Te sensors provide fairly stable results, whereas for the St sensors, it really depends on the location whether they can be use reliably. Specifically, sensors inside the deck, oriented horizontally on the left side of the bridge[2], appear to work well. Note

that such observations are highly useful for the design of future sensor networks, as it provides guidelines to the effective placement of a small collection of sensors. Although subgroups 4 to 8 provide some information as to the placement of Te sensors, these subgroups are not radically different from 'St vertical = inside deck', and have a slightly lower quality (although sometimes higher μ_{S_i}).

St-Vi models Table 3 presents the top-9 subgroups for the strain and vibration models. The results present a much more balanced picture, with both St and Vi properties being crucial for a reliable model. Clearly, the location of sensors at the girders provides the best results, an observation that is corroborated by civil engineering experts in the project. Note that either side of the bridge is much more useful for St placement, compared to the middle of the bridge. We also identify several individual strain sensors (St1, St11, St83) located on both sides of the bridge that play a useful role in many models they feature in. Note that these selected sensors correspond to the three darkest columns in the correlation matrix in Fig. 1 (right).

7. Conclusion and future work

We have demonstrated the use of a number of key data mining and signal processing techniques to model dependencies among multiple sensor types. We have built a linear model to correlate strain and tempera-

---

[2]The bridge was under construction during this period, and was not being use symmetrically.

Table 3. The $d \leq 2$ results for the St-Vi models ($\mu_0 = 0.139$).

SUBGROUP DESCRIPTION	COVERAGE %	z-SCORE	μ_{S_i}
ST VERTICAL = GIRDER	17.4	31.3	0.36
VI VERTICAL = GIRDER & ST VERTICAL = GIRDER	10.2	28.0	0.40
ST VERTICAL = GIRDER & ST HORIZONTAL = RIGHT	6.5	24.8	0.43
ST EMBEDDING = ATTACH & ST ORIENTATION = X-AXIS	38.0	17.7	0.21
ST VERTICAL = GIRDER & VI VERTICAL = UNDER DECK	7.2	15.3	0.31
SENSOR = ST1 & VI VERTICAL = GIRDER	0.6	12.8	0.62
ST VERTICAL = GIRDER & ST HORIZONTAL = LEFT	6.5	12.2	0.28
SENSOR = ST83 & VI VERTICAL = GIRDER	0.6	11.4	0.56
SENSOR = ST11 & VI HORIZONTAL = RIGHT	0.4	11.4	0.68

ture readings, and improved this model through convolution with an exponential response function. In the frequency domain, we used band-pass filters to detect the correlated spectra between strain and vibration sensor time series. For modeling dependencies between vibration and temperature sensor time series, the modes of the spectrum were identified. We note that most low frequency modes are affected little by temperature changes. Finally, we conducted secondary analysis of the models obtained in Section 3 and 4, and extracted subgroups to explain the effects of sensor placement. The extracted rules can be used as guidelines for designing more (cost-)effective networks on future Structural Health Monitoring installations.

References

Hespanha, J. (2009). *Linear system theory*. Princeton university press.

Knobbe, A., Blockeel, H., Koopman, A., Calders, T., Obladen, B., Bosma, C., Galenkamp, H., Koenders, E., & Kok, J. (2010). InfraWatch: Data management of large systems for monitoring infrastructural performance. *Proceedings of Intelligent Data Analysis* (pp. 91–102).

Liu, C., & Dewolf, J. T. (2007). Effect of temperature on modal variability of a curved concrete bridge under ambient loads. *Journal of structural engineering, 133*, 1742–1751.

Meeng, M., & Knobbe, A. (2011). Flexible Enrichment with Cortana - Software Demo. *the 20th Machine Learning conference of Belgium and The Netherlands.*

Miao, S., Knobbe, A., Koenders, E., & Bosma, C. (2013). Analysis of traffic effects on a dutch highway bridge. *Proceedings of IABSE.*

Peeters, B., & De Roeck, G. (2000). One-year monitoring of the Z24-bridge: environmental effects versus damage events. *Proceedings of IMAC 18, the International Modal Analysis Conference* (pp. 1570–1576).

Pieters, B., Knobbe, A., & Džeroski, S. (2010). Subgroup discovery in ranked data, with an application to gene set enrichment. *Proceedings of PL 2010 at ECML PKDD.*

Reynolds, P., & Pavic, A. (2001). Comparison of forced and ambient vibration measurements on a bridge. *Proceedings of the International Modal Analysis Conference IMAC, 1*, 846–851.

Song, W., & Dyke, S. (2006). Ambient vibration based modal identification of the Emerson bridge considering temperature effects. *The 4th world conference on structural control and monitoring.*

Stranneby, D., & Walker, W. (2004). *Digital signal processing and applications.* Elsevier.

Vespier, U., Knobbe, A., Vanschoren, J., Miao, S., Koopman, A., Obladen, B., & Bosma, C. (2011). Traffic Events Modeling for Structural Health Monitoring. *Proceedings of Intelligent Data Analysis.*

Xia, Y., Hao, H., Zanardo, G., & Deeks, A. (2006). Long term vibration monitoring of an RC slab: temperature and humidity effect. *Engineering Structures* (pp. 441–452).

Xia, Y., Weng, S., Su, J., & Xu, Y. (2011). Temperature effect on variation of structural frequencies: from laboratory testing to field monitoring. *The 6th International Workshop on Advanced Smart Materials and Smart Structures Technology.*